INTERNATIONAL JOURNAL FOR NUMERICAL AND ANALYTICAL METHODS IN GEOMECHANICS, VOL. 21, 549–568 (1997)

BEHAVIOR OF CEMENTED SANDS—II. MODELLING

ALI A. ABDULLA*,[1] AND PANOS D. KIOUSIS†,§,[2]

[1]*Ministry of Health, Muscat, Sultanate of Oman*
[2]*Department of Civil Engineering and Engineering Mechanics, The University of Arizona, Tucson, AZ 85721, U.S.A.*

SUMMARY

This is the companion paper to a study the triaxial testing of cemented sands. The focus here is turned to the constitutive modelling of cemented sands. A novel micromechanical approach that considers the multi-phase nature of cemented sands, is presented in which the clean sand, the cementing bond and the pore water pressure are modelled independently. The model is verified using a series of triaxial compression experiments on 2, 4 and 6 per cent cemented specimens, that were the subject of the companion paper. © 1997 by John Wiley & Sons, Ltd.

Int. J. Numer. Anal. Meth. Geomech., Vol. 21, 549–568 (1997)
(No. of Figures: 14 No. of Tables: 3 No. of Refs: 20)

Key words: cemented sand; constitutive model; multiphase material; strength; dilatancy

INTRODUCTION

Soil cementation, artificial and natural, has been investigated extensively by geotechnical engineers due to its significant effects on the soil strength and stiffness characteristics. Research efforts that highlight the importance of cemented soils are reviewed in the companion paper,[1] which concentrates on the triaxial testing of cemented soils. In this paper, the focus is placed on the modelling of the stress–strain behaviour of cemented sands.

The multi-phase nature of cemented soils, consisting of soil, cement and pore water, requires a more fundamental, microchemical framework for model development. In this study, a novel constitutive model is presented that is generated from the synthesis of the individual constituents of a cemented soil. The microchemical development presented here is equivalent to a mixture-based approach and provides a natural tool to quantify the material degradation caused by cementation breakage during loading.

BACKGROUND

Most published studies on cemented soils concentrate on the experimental procedures necessary to develop failure criteria.[2–7] The usefulness of accurate failure criteria to define failure stress relations is undisputed. However, such criteria do not provide any information on the

* Project Director. Formerly, Graduate Student, Department of Civil Engineering and Engineering Mechanics,The University of Arizona, Tucson, AZ 85721, U.S.A.
† Associate Professor.
§ Correspondence to P. D. Kiousis, Department of Civil Engineering and Engineering Mechanics, The University of Arizona, Tucson, AZ 87521, U.S.A.

CCC 0363–9061/97/080549–20$17.50

Received 30 May 1996
Revised 26 November 1996

stress–strain relations of these materials before and after failure. Constitutive models that provide stress–strain relations for soils are rather abundant, but have not been concerned with cemented soils.[8–11] Exceptions to this rule are the works of Hirai *et al.*,[12] Pekau and Gocevski[13] and Desai and coworkers.[14,15] These models have been developed based on concepts on a homogeneous one-phase material. Thus, even though they produce the general trend of deformation characteristics of cemented sands, they are not able to capture the special mechanisms that lead to the degradation and eventual failure of the sand–cement composite.

The present study aims to overcome such modelling deficiencies by developing a constitutive model that captures the mechanics of deformation and degradation of cemented sand, and is simple enough to provide a useful tool that can be implemented in finite element codes for the analysis of foundation problems on cemented sands.

DEVELOPMENT OF A GENERAL CONSTITUTIVE MODEL

The constitutive model that is presented here is based on the following principles:

1. A cemented sand specimen is viewed from the outset as a composite material or *mixture* with three phases: sand, cement and pore water.
2. The elastoplastic behaviour of a cemented sand is the result of the following:
   (a) The elastoplastic response of the sand.
   (b) The elastoplastic response of the cementing bonds *before they break*.
   (c) The interaction between the phases.
   (d) The breaking of the cement bonds.
3. The models of the individual phases are assembled, using micromechanical equilibrium, to predict the overall behaviour of cemented sands.

Global material equations—the micromechanical model

Consider the contact of two grains of a saturated cemented sand (Figure 1). The load transfer between the two grains is obtained partly through the inter-grain contact area A_t, and partly through the cemented areas A_1 and A_2, The equilibrium of the forces results in the following equation:

$$P = P_t + P_1 + P_2 + u(A - A_1 - A_2 - A_t) \tag{1}$$

where A is the total area, P_t the force transferred through the grain contact, P_1 and P_2 the forces transferred through cementation, u the fluid pressure, and $u(A - A_1 - A_2 - A_t)$ the force carried by the pore fluid.

Division of equation (1) throughout by A results in

$$\frac{P}{A} = \frac{P_t}{A} + \frac{P_1 + P_2}{A} + u\left(1 - \frac{A_1 + A_2}{A} - \frac{A_t}{A}\right) \tag{2}$$

or

$$\frac{P}{A} = \frac{P_t}{A} + \frac{P_1 + P_2}{A_1 + A_2}\frac{A_1 + A_2}{A} + u\left(1 - \frac{A_1 + A_2}{A} - \frac{A_t}{A}\right) \tag{3}$$

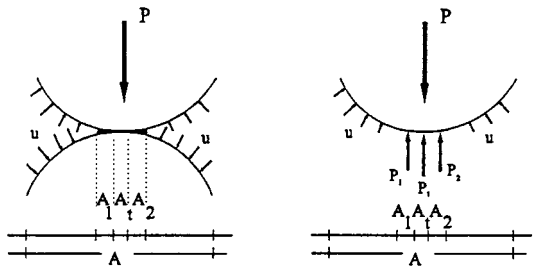

Figure 1. Model for micromechanical stress analysis

or

$$\sigma = \sigma' + \sigma_c n_c + u\left(1 - n_c - \frac{A_t}{A}\right) \tag{4}$$

where σ is the total stress, σ' the effective stress, σ_c is the intrinsic (true) stress of the cementation, $n_c = (A_1 + A_2)/A$, and the grain contact proportion A_t/A is commonly considered negligible and can be omitted:

$$\sigma = \sigma' + \sigma_c n_c + u(1 - n_c) \tag{5}$$

For a statistically isotropic soil, n_c can be written as[16]

$$n_c = \frac{dV_c}{dV} \tag{6}$$

where V_c is the volume occupied by the cement phase and V is the total material volume. Based on the definition of equation (6), n_c is the volumetric cement content.

Equation (5) can also be produced using a homogenized theory of mixtures.[17] Equation (5) can be extended to its three-dimensional tensor equivalent, and can be written incrementally as follows:

$$d\boldsymbol{\sigma} = d\boldsymbol{\sigma}' + n_c d\boldsymbol{\sigma}_c + dn_c \boldsymbol{\sigma}_c + (1 - n_c) d\mathbf{u} - dn_c \mathbf{u} \tag{7}$$

Each incremental quantity in equation (7) can be defined by an appropriate constitutive model:

$$d\boldsymbol{\sigma}' = \mathbf{D}_s \cdot d\boldsymbol{\varepsilon} \tag{8}$$

$$d\boldsymbol{\sigma}_c = \mathbf{D}_c \cdot d\boldsymbol{\varepsilon} \tag{9}$$

$$d\mathbf{u} = \mathbf{D}_w \cdot d\boldsymbol{\varepsilon} \tag{10}$$

$$dn_c = \mathbf{S}^T \cdot d\boldsymbol{\varepsilon} \tag{11}$$

It is assumed that no diffusion takes place, and thus all phases of the mixture have the same strains. However, the elastic and plastic components of the strain tensor are not the same for all phases. Substitution of equations (8)–(11) into equation (7) results in

$$d\boldsymbol{\sigma} = \mathbf{D} \cdot d\boldsymbol{\varepsilon} \tag{12}$$

where $\mathbf{D}$ is the *global* constitutive matrix and is defined as

$$\mathbf{D} = \mathbf{D}_s + n_c\mathbf{D}_c + \boldsymbol{\sigma}_c\mathbf{S}^T + (1 - n_c)\mathbf{D}_w - \mathbf{u}\,\mathbf{S}^T \tag{13}$$

For drained or dry conditions, equation (13) reduces to

$$\mathbf{D} = \mathbf{D}_s + n_c\mathbf{D}_c + \boldsymbol{\sigma}_c\mathbf{S}^T \tag{14}$$

Thus, the global constitutive matrix of the cemented sand mixture is developed from the constitutive matrices of its individual components, defined by equations (8)–(11). With the exception of equation (11), these expressions are rather common within the field of plasticity modelling. Equation (11) is an expression of the degradation of the cementation (i.e. reduction of the cementation content) due to bond breakage. The development of the components of equation (14) is presented in the following three sections. The constitutive laws that are used here to model the responses of the individual components are chosen purposely to be fairly simple to avoid detracting attention from the main contribution, which is the 'micromechanical binder' (i.e. equations (5) and (13)).

Sand modelling

A simple, Drucker–Prager-type plasticity model, with non-associative isotropic hardening is adopted for the sand phase. A brief description of the model follows:

Loading surface:

$$F_s = \sqrt{J_{2D}} - \alpha_s(\hat{\varepsilon}_s)J_1 = 0 \tag{15}$$

where α_s is an isotropic hardening function given by

$$\alpha_s(\hat{\varepsilon}_s) = a_s^0 + \frac{\hat{\varepsilon}_s}{(1/E_s^a) + \hat{\varepsilon}_s/(a_s^{ult} - \alpha_s^0)} \tag{16}$$

and α_s^0, E_s^a, and α_s^{ult} are material parameters of the soil phase. $\hat{\varepsilon}_s$ is the plastic strain trajectory of the soil phase defined as

$$\hat{\varepsilon}_s = \int \sqrt{\mathrm{d}\boldsymbol{\varepsilon}_s^p\,\mathrm{d}\boldsymbol{\varepsilon}_s^p} \tag{17}$$

where $\mathrm{d}\boldsymbol{\varepsilon}_s^p$ is the incremental plastic strain tensor of the soil phase.

Potential surface:

$$G_s = \sqrt{J_{2D}} - \beta_s(\sigma_3)J_1 \tag{18}$$

where β_s is dilation parameter.

Flow rule:

$$\mathrm{d}\boldsymbol{\varepsilon}^p = \mathrm{d}\lambda_s \frac{\partial G_s}{\partial \boldsymbol{\sigma}'} \tag{19}$$

Constitutive matrix:

Following standard plasticity procedures we find[17]

$$\mathrm{d}\boldsymbol{\sigma}' = \mathbf{D}_\mathrm{s}\,\mathrm{d}\boldsymbol{\varepsilon} \tag{20}$$

where

$$\mathbf{D}_\mathrm{s} = \mathbf{E}_\mathrm{s} - \frac{\mathbf{E}_\mathrm{s}\dfrac{\partial G_\mathrm{s}}{\partial \boldsymbol{\sigma}'}\dfrac{\partial F_\mathrm{s}^\mathrm{T}}{\partial \boldsymbol{\sigma}'}\mathbf{E}_\mathrm{s}}{\dfrac{\partial F_\mathrm{s}^\mathrm{T}}{\partial \boldsymbol{\sigma}'}\mathbf{E}_\mathrm{s}\dfrac{\partial G_\mathrm{s}}{\partial \boldsymbol{\sigma}'} + J_1\dfrac{\partial \alpha}{\partial \hat{\varepsilon}_\mathrm{s}}\sqrt{\dfrac{\partial G_\mathrm{s}^\mathrm{T}}{\partial \boldsymbol{\sigma}'}\dfrac{\partial G_\mathrm{s}}{\partial \boldsymbol{\sigma}'}}} \tag{21}$$

Cement modelling

A simple, non-associative, isotropicly hardening von Mises plasticity model is adopted for the cement phase. A brief description of the model follows:

Loading surface:

$$F_\mathrm{c} = \sqrt{J_{2\mathrm{D}}} - \alpha_\mathrm{c}(\hat{\varepsilon}_\mathrm{c}) = 0 \tag{22}$$

where α_c is an isotropic hardening function given by

$$\alpha_\mathrm{c} = a_\mathrm{c}^0 + \frac{\hat{\varepsilon}_\mathrm{c}}{(1/(\sqrt{2}/3)E_\mathrm{c}^\mathrm{a}) + \hat{\varepsilon}_\mathrm{c}/(a_\mathrm{c}^\mathrm{ult} - \alpha_\mathrm{c}^0)} \tag{23}$$

where α_c^0, E_c^a, and $\alpha_\mathrm{c}^\mathrm{ult}$ are material parameters of the soil phase, $\hat{\varepsilon}_\mathrm{c}$ is the plastic strain trajectory of the cement phase defined as

$$\hat{\varepsilon}_\mathrm{c} = \int \sqrt{\mathrm{d}\boldsymbol{\varepsilon}_\mathrm{c}^\mathrm{p}\,\mathrm{d}\boldsymbol{\varepsilon}_\mathrm{c}^\mathrm{p}} \tag{24}$$

where $\mathrm{d}\boldsymbol{\varepsilon}_\mathrm{c}^\mathrm{p}$ is the incremental plastic strain tensor of the soil phase.

Potential surface:

$$G_\mathrm{c} = \sqrt{J_{2\mathrm{D}}} - \beta_\mathrm{c}(\sigma_3)J_1 \tag{25}$$

where β_c is a dilation parameter. Cemented sands under shearing often tend to compress more than clean sands. This is because cemented particles are originally kept apart by cementation. During shearing, cementation breaks and allows particles to approach each other resulting in larger initial volumetric compression. The parameter β_c is designed to produce this compressive behaviour and is discussed in detail in the section for the evaluation of the material parameters.

Flow rule:

$$\mathrm{d}\boldsymbol{\varepsilon}^\mathrm{p} = \mathrm{d}\lambda_\mathrm{c}\frac{\partial G_\mathrm{c}}{\partial \boldsymbol{\sigma}_\mathrm{c}} \tag{26}$$

Constitutive matrix:

Following standard plasticity procedures we find[17]

$$\mathrm{d}\boldsymbol{\sigma}_\mathrm{c} = \mathbf{D}_\mathrm{c}\,\mathrm{d}\boldsymbol{\varepsilon} \tag{27}$$

where

$$\mathbf{D}_\mathrm{c} = \mathbf{E}_\mathrm{c} - \frac{\mathbf{E}_\mathrm{c}\dfrac{\partial G_\mathrm{c}}{\partial \boldsymbol{\sigma}_\mathrm{c}}\dfrac{\partial F_\mathrm{c}^\mathrm{T}}{\partial \boldsymbol{\sigma}_\mathrm{c}}\mathbf{E}_\mathrm{c}}{\dfrac{\partial F_\mathrm{c}^\mathrm{T}}{\partial \boldsymbol{\sigma}_\mathrm{c}}\mathbf{E}_\mathrm{c}\dfrac{\partial G_\mathrm{c}}{\partial \boldsymbol{\sigma}_\mathrm{c}} + \dfrac{\partial \alpha}{\partial \hat{\varepsilon}_\mathrm{c}}\sqrt{\dfrac{\partial G_\mathrm{c}^\mathrm{T}}{\partial \boldsymbol{\sigma}_\mathrm{c}}\dfrac{\partial G_\mathrm{c}}{\partial \boldsymbol{\sigma}_\mathrm{c}}}} \tag{28}$$

Cementation degradation

The gradual breakage of the cement bonds within the soil mass is modelled by equation (11). The hypothesis adopted for the reduction in cementation is expressed mathematically by the exponential decay equation

$$n_\mathrm{c} = n_{\mathrm{c}0}\exp(-\theta\hat{\varepsilon}_\mathrm{c}) \tag{29}$$

where $n_{\mathrm{c}0}$ is the initial volumetric content of the undamaged cementation, n_c is the current volumetric content of the undamaged cementation and θ is a material degradation parameter.

The incremental form of (29) is written as

$$\mathrm{d}n_\mathrm{c} = -n_{\mathrm{c}0}\theta\exp(-\theta\hat{\varepsilon}_\mathrm{c})\,\mathrm{d}\hat{\varepsilon}_\mathrm{c} \tag{30}$$

Using the definition of $\hat{\varepsilon}_\mathrm{c}$ (equation (24)) and the flow rule (equation (26)) we find

$$\mathrm{d}\hat{\varepsilon}_\mathrm{c} = \mathrm{d}\lambda_\mathrm{c}\sqrt{\frac{\partial G_\mathrm{c}^\mathrm{T}}{\partial \boldsymbol{\sigma}_\mathrm{c}}\frac{\partial G_\mathrm{c}}{\partial \boldsymbol{\sigma}_\mathrm{c}}} \tag{31}$$

which results in

$$\mathrm{d}n_\mathrm{c} = \mathbf{S}^\mathrm{T}\,\mathrm{d}\boldsymbol{\varepsilon} \tag{32}$$

where

$$\mathbf{S}^\mathrm{T} = \frac{-n_{\mathrm{c}0}\theta\exp(-\theta\hat{\varepsilon}_\mathrm{c})\sqrt{\dfrac{\partial G_\mathrm{s}^\mathrm{T}}{\partial \boldsymbol{\sigma}_\mathrm{c}}\dfrac{\partial G_\mathrm{s}}{\partial \boldsymbol{\sigma}_\mathrm{c}}}\dfrac{\partial G_\mathrm{s}^\mathrm{T}}{\partial \sigma_\mathrm{c}}\mathbf{E}_\mathrm{c}}{\dfrac{\partial F_\mathrm{s}^\mathrm{T}}{\partial \boldsymbol{\sigma}_\mathrm{c}}\mathbf{E}_\mathrm{c}\dfrac{\partial G_\mathrm{s}^\mathrm{T}}{\partial \boldsymbol{\sigma}_\mathrm{c}} + \dfrac{\mathrm{d}\alpha^\mathrm{c}}{\mathrm{d}\hat{\varepsilon}_\mathrm{c}}\sqrt{\dfrac{\partial G_\mathrm{s}^\mathrm{T}}{\partial \boldsymbol{\sigma}_\mathrm{c}}\dfrac{\partial G_\mathrm{s}}{\partial \boldsymbol{\sigma}_\mathrm{c}}}} \tag{33}$$

EVALUATION OF MATERIAL PARAMETERS

Material parameters of sand

The sand is modelled as an elastoplastic hardening material. The material parameters associated with the model are:

(a) Elastic parameters: E_s and ν_s
(b) Loading surface and hardening parameters: α_s^0, E_s^a and $\alpha_\mathrm{s}^\mathrm{ult}$
(c) Dilation rate parameter: β_s

The *elastic modulus* E_s is expressed as a function of the confinement:[18]

$$E_s = KP_a\left[\frac{\sigma'_3}{P_a}\right]^n \tag{34}$$

Calculation of the elastic parameters is straightforward and is not discussed here.

The loading surface, equation (15), can be rewritten as follows for the triaxial test:

$$\alpha_s = \frac{\sqrt{J_{2D}}}{J_1} = \frac{\sigma_1 - \sigma_3}{\sqrt{3}(\sigma_1 + 2\sigma_3)} \tag{35}$$

Substitution of equation (16) into equation (35) provides a relation between $\hat{\varepsilon}$ and σ_1, which is a function of the confining pressure σ_3 and the hardening constants α_s^0 and α_s^{ult}, which are calculated using curve-fitting, as shown in Figure 2.

The *dilation parameter* β_s is expressed as a function of confinement also:

$$\beta_s = \beta_s^0 \exp(-\beta_s^p \sigma'_3) \tag{36}$$

where β_s^0 and β_s^p are constants to be calculated. To evaluate these constants, the *experimental dilation rate* parameter ψ_s is introduced as

$$\psi_s = \frac{dI_1^p}{d\sqrt{I_{2D}^p}} \tag{37}$$

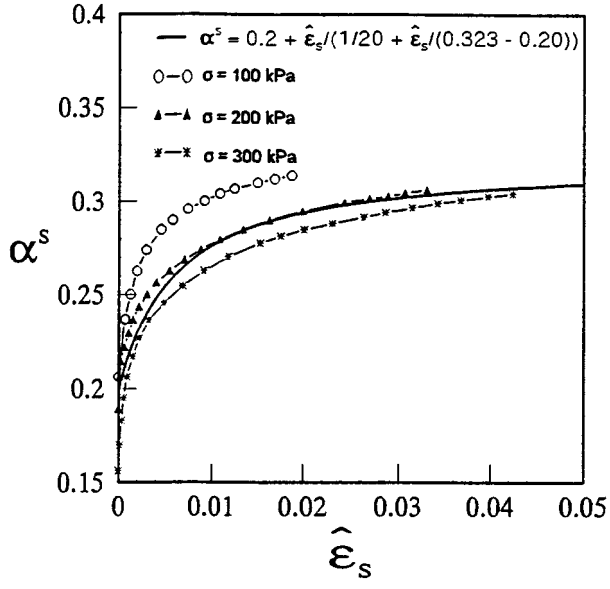

Figure 2. Loading surface parameters for the sand phase

where I_1^p is the first invariant of the plastic strain tensor, and I_{2D}^p is the second invariant of the deviatoric plastic strain tensor. For a triaxial test, equation (37) takes the form

$$\psi_s = \frac{d\varepsilon_1^p + 2d\varepsilon_3^p}{(1/\sqrt{3})(d\varepsilon_1^p - d\varepsilon_3^p)} \tag{38}$$

Equation (38), combined with the flow rule (19), results in[17]

$$\beta_s = \frac{\psi_s}{6} \tag{39}$$

Thus, β_s^0 and β_s^p are found from data fitting of the volumetric strain rates of sand under various confinement stresses. For the sands tested here, the material parameters are listed in Table I.

Material parameters of the cement phase

The cement phase is also modelled as an elastoplastic hardening material. The cement phase is unique in the sense that it is a sparse, probably discontinuous material in the composite. For the case of a soil with 6 per cent cementation, the volumetric content of the cement is $n_c \approx 0{\cdot}03$.* The second important feature of the cement phase is that it breaks during shearing resulting in an even smaller value of n_c. In essence, cementation acts as a series of uniaxially loaded micro-columns distributed arbitrarily in space, statistically in all directions, producing an apparently isotropic response that is modelled as a very porous material. The parameters needed to evaluate the cement behaviour are:

1. elastic parameters: E_c and v_c.
2. initial cementation: n_{c0}.
3. loading surface and hardening parameters: α_c^0, α_c^{ult} and E_c^a.
4. Damage parameter θ.
5. Compression coefficient β_c.

Most cement parameters can be obtained from a simple compression test of a cement specimen. However, it is easier, and more useful to derive the cement parameters from a cemented soil specimen. For this purpose, a simple unconfined compression test on a cemented sand is sufficient. Since sandy soils have no strength under zero confinement, the general equation of stresses under dry conditions,

$$\sigma = \sigma' + n_c\sigma_c \tag{40}$$

becomes

$$\sigma = n_c\sigma_c \tag{41}$$

or, for a unconfined compression test,

$$\sigma_1 = n_c\sigma_{c1} \tag{42}$$

* This is not an obvious conclusion and is explained later in equation (44)

Table I. Soil materials parameters

Elastic parameters			Loading/hardening parameters			Dilation parameters	
K	n	ν_s	α_s^0	α_s^{ult}	E_s^a	β_s^0	β_s^p
3.4 MPa or 497 psi	0·51	0·29	0·2	0·323	20	0·16	0·02

where σ_1 is the total stress applied on the specimen, and σ_{c1} is the intrinsic stress on the cement phase.

The *modulus of elasticity* E_c can be found from (42) as

$$E_c = \frac{E}{n_{c0}} \tag{43}$$

where E is the modulus of elasticity of the cemented soil, calculated from an unconfined compression test.

To evaluate the *initial cementation* value n_{c0} the following relation, derived from a simple phase diagram, is used:[17]

$$n_{c0} = \omega_c \frac{\rho_d}{\rho_c} \tag{44}$$

where ω_c is the percent of cement content by total weight of dry soil (sand and cement), ρ_c the density of cement and ρ_d the dry density of the cemented soil.

The *loading surface and hardening* coefficients of α_c are also evaluated from an unconfined compression test of the cemented soil. A typical uniaxial stress–strain relation of a cemented soil is shown in Figure 3. The yield point A is characterized by the initiation of bond breakage and plastic deformations, i.e. at $A : n_c = n_{c0}$ and $\hat{\varepsilon} = 0$. Based on equations (22) and (23) is is found that for point A,

$$\alpha_c^0 = \frac{\sigma_1^y}{\sqrt{3} n_{c0}} \tag{45}$$

The peak point B is used to determine α_c^{ult} as

$$\alpha_c^{ult} = \frac{\sigma_1^{ult}}{\sqrt{3} n_c} \tag{46}$$

The evaluation of α_c^{ult} requires the value of n_c at point B, which is not equal to n_{c0} due to the inelastic deformations and cementation degradation between points A and B. There seems to be no direct way to calculate accurately the value of n_c at point B. However, numerous indirect estimations of n_c at point B[17] resulted in $n_c = 0{\cdot}95 n_{c0}$. Thus, equation (46) is rewritten as

$$\alpha_c^{ult} = \frac{\sigma_1^{ult}}{\sqrt{3}\, 0{\cdot}95 n_{c0}} \tag{47}$$

The *compression* parameter β_c is calculated from $\beta_c = -\psi_c/6$, where

$$\psi_c = \frac{dI_1^p}{d\sqrt{I_{2D}^p}} \tag{48}$$

The purpose of β_c is to control the plastic deformations of the cement phase and ensure exhibition of the initial compressive behaviour. To evaluate β_c one must understand the deformation characteristics of the cemented soils. During an *unconfined* compression test of a cemented sand, strains ε_1 and ε_3 are recorded. Assuming equal total strains on all constituents we can write

$$\varepsilon_1 = \varepsilon_{c1}^e + \varepsilon_{c1}^p = \varepsilon_{s1}^e + \varepsilon_{s1}^p \tag{49}$$

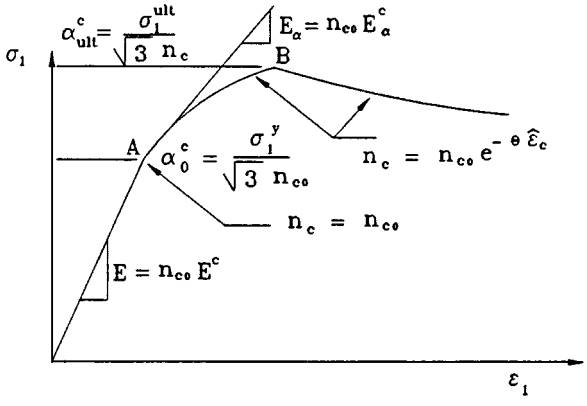

Figure 3. Typical uniaxial stress–strain schematic for cemented sands

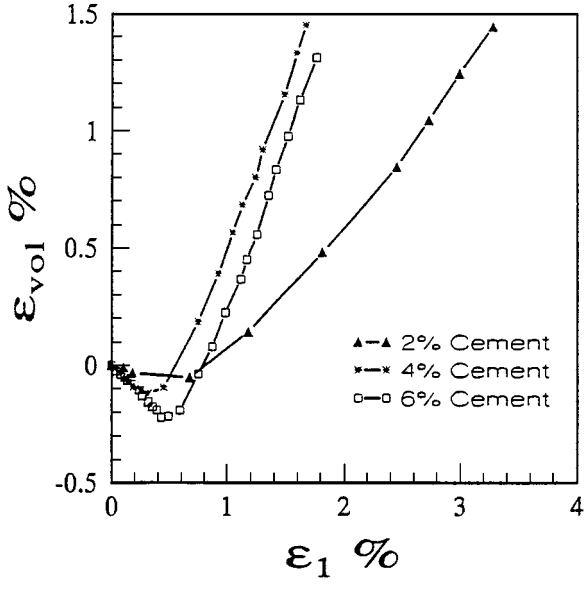

Figure 4. Volumetric strain response for cemented sand as a function of cementation

and

$$\varepsilon_3 = \varepsilon^{\mathrm{e}}_{\mathrm{c}3} + \varepsilon^{\mathrm{p}}_{\mathrm{c}3} = \varepsilon^{\mathrm{e}}_{\mathrm{s}3} + \varepsilon^{\mathrm{p}}_{\mathrm{s}3} \tag{50}$$

Since the test is unconfined, the sand carries no stresses; thus, $\varepsilon^{\mathrm{p}}_{\mathrm{s}} = \varepsilon$ and $\varepsilon^{\mathrm{e}}_{\mathrm{s}} = 0$. At the latter stages of shearing, when the cementation breaks down, the sand deformations dominate the overall behaviour. During the early stages of deformation however, and especially before the peak stress development, the deformation of the cement dominates the behaviour of the mixture. The values of β_{c} therefore should be such that they can adequately describe the volumetric characteristics of the mixture at the early stages. Thus, β_{c} should express the high compression rate of the cemented sand specimen in the beginning of the shearing, which decreases to zero during the post-peak shearing. The following function is chosen:[16]

$$\beta_{\mathrm{c}} = \frac{1}{6E^{\beta}_{\mathrm{c}}} \frac{1}{\left[\dfrac{1}{E^{\beta}_{\mathrm{c}}} + \dfrac{\sqrt{I^{\mathrm{p}}_{2\mathrm{D}}}}{\Delta^{\beta}_{\mathrm{c}}}\right]^2} \tag{51}$$

where E^{β}_{c} is the initial slope of β_{c} and $\Delta^{\beta}_{\mathrm{c}}$ is the ultimate value of β_{c}.

The *damage or degradation* coefficient θ (equation (29)) is also determined from the peak strength of the cemented soil, and is based on the experimental observation that the stresses of the cement bonds peak at about the same strength for the same cement content regardless of the value of the confining pressure.[19] The procedure to determine θ by tabulation is presented in Table II.

The experimental data obtained in this study provide very consistent values for θ *in the post-peak region.* These are listed in Table III. For the initial stages of plastic deformation, θ varies from initial values as high as 40, which rapidly reduces to approximately zero, and then increases to the final values listed in Table III. However, it was found through numerical experiments that the material response predictions are insensitive to the initial values of θ, and, thus, use of the constant post-peak value of θ was assumed adequate.

Table II. Calculation of parameters h

1	2	3	4	5	6	7	8	9	10
ε_1	σ_1	$\sigma_1/n_{\mathrm{c}0}$	$\varepsilon^{\mathrm{e}}_1$	$\varepsilon^{\mathrm{p}}_1$	σ^{c}_1	$\dfrac{n_{\mathrm{c}}}{n_{\mathrm{c}0}}$	$\ln \dfrac{n_{\mathrm{c}}}{n_{\mathrm{c}0}}$	$\hat{\varepsilon}_{\mathrm{c}}$	θ

Note: The parameters are as defined below

ε_1	the measured axial strain from the unconfined compression test
σ_1	the measured axial stress from the unconfined compression test
$\sigma_1/n_{\mathrm{c}0}$	normalized axial stress $= (n_{\mathrm{c}} \cdot \sigma^{\mathrm{c}}_1)/n_{\mathrm{c}0}$
$\varepsilon^{\mathrm{e}}_1$	calculated elastic strain $(= (\sigma_1/E))$
$\varepsilon^{\mathrm{p}}_1$	calculated plastic strain $(= \varepsilon_1 - \varepsilon^{\mathrm{e}}_1)$
σ^{c}_1	calculated axial stress of *undamaged cement*. From the constitutive equations (22) and (23), specialized for the unconfined compression test
$n_{\mathrm{c}}/n_{\mathrm{c}0}$	ratio of current undegraded cementation to initial cementation (= (column 3)/(column 6))
$\hat{\varepsilon}_{\mathrm{c}}$	plastic strain trajectory for the unconfined compression test $(= \varepsilon^{\mathrm{p}}_1 \sqrt{(\xi - 1)^2/2})$ where ξ is the dilation coefficient measured from the volumetric strain response of the unconfined compression test. It is defined as the slope of the $\varepsilon^{\mathrm{p}}_{\mathrm{vol}}$ vs. $\varepsilon^{\mathrm{p}}_1$ diagram. Note that $\xi > 0$ for compression and $\xi < 0$ for dilatation. For the tests examined here (Figure 4) ξ is calculated to be equal to $-1{\cdot}25$ for 4 and 6 per cent cementation. For 2 per cent cementation $\xi = -0{\cdot}6$
θ	$-(\ln n_{\mathrm{c}} - \ln n_{\mathrm{c}0})/\hat{\varepsilon}_{\mathrm{c}}$

Table III. Cement material parameters

Cement content	E	n_{c0}	θ	α_c^0	α_c^{ult}	E^α	E_c^β	Δ_c^β
2%	8500 psi 56·6 MPa	0·0095	4·1	186 psi 1·3 MPa	1640 psi 11·3 MPa	6000 psi 41·3 MPa	1·3	0·012
4%	16,600 psi 114·4 MPa	0·0194	5·2	1234 psi 8·5 MPa	2404 psi 16·6 MPa	15,000 psi 103·4 MPa	1·3	0·012
6%	20,000 psi 137·8 MPa	0·0307	6·0	1840 psi 12·7 MPa	3355 psi 23·1 MPa	24,000 psi 165·4 MPa	1·3	0·012

In summary, the material parameters of the cement phase can be obtained from a simple unconfined compression test. For the cement specimens tested here the parameters as given in Table III are found.

COMPUTER IMPLEMENTATION

The plasticity constitutive equations are often too complex to integrate analytically, leading to numerical integration schemes. The basics of these schemes are well established and are not discussed here. However, some difficult and unique problems in the integration of a multi-phase materials exist, and merit further discussion.

Global equilibrium

The problem of constitutive relations for the triaxial compression test is described as follows:

For N steps:
GIVEN: $\sigma'_1, \sigma'_2, \sigma'_3, \sigma_{c1}, \sigma_{c2}, \sigma_{c3}, \varepsilon_1, \varepsilon_2, \varepsilon_3$, and $\Delta\sigma_2, \Delta\sigma_3, \Delta\varepsilon_1$
SOLVE FOR: $\Delta\varepsilon_2, \Delta\varepsilon_3, \Delta\sigma_1$ as well as $\Delta\sigma'_1, \Delta\sigma'_2, \Delta\sigma'_3, \Delta\sigma_{c1}, \Delta\sigma_{c2}$, and $\Delta\sigma_1$.

The numerical integration of the constitutive equations for a single-phase material is straightforward. However, multi-phase plasticity relations are more complex and their integration is subjected to additional constraints. The procedures developed here are listed as follows:

STEP 0: At the end of the jth increment, the state of stress and strain of each phase is known. That is, $\sigma'_1, \sigma'_2, \sigma'_3, \sigma_{c1}, \sigma_{c2}, \sigma_{c3}$ and $\varepsilon_1, \varepsilon_2, \varepsilon_3$ are known.

STEP 1: The global incremental equations (12) are rearranged to express the known boundary conditions:

$$\begin{bmatrix} D_{22} & D_{23} \\ D_{32} & D_{33} \end{bmatrix} \cdot \begin{Bmatrix} \Delta\varepsilon_2 \\ \Delta\varepsilon_3 \end{Bmatrix} = \begin{Bmatrix} \Delta\sigma_2 - \Delta_{21} & \Delta\varepsilon_1 \\ \Delta\sigma_3 - D_{31} & \Delta\varepsilon_1 \end{Bmatrix}$$

and (52)

$$\Delta\sigma_1 = D_{11}\Delta\varepsilon_1 + D_{12}\Delta\varepsilon_2 + D_{13}\Delta\varepsilon_3$$

The first part of equations (52) is solved for $\Delta\varepsilon_2$ and $\Delta\varepsilon_3$. The stress increment $\Delta\sigma_1$ is evaluated subsequently from the second part of equations (52).

STEP 2: With all strain increments $\Delta\varepsilon_1$, $\Delta\varepsilon_2$, and $\Delta\varepsilon_3$ known, equations (8) and (9), combined with a radial mapping return algorithm, are used to evaluate the stress increments of the soil skeleton and the cement phase, respectively.

STEP 3: The cumulative stresses are calculated next:

$$\sigma'_1 \leftarrow \sigma'_1 + \Delta\sigma'_1;\ \sigma'_2 \leftarrow \sigma'_2 + \Delta\sigma'_2;\ \sigma_3 \leftarrow \sigma_3 + \Delta\sigma_3$$

$$\sigma_{c1} \leftarrow \sigma_{c1} + \Delta\sigma_{c1};\ \sigma_{c2} \leftarrow \sigma_{c2} + \Delta\sigma_{c2};\ \sigma_{c3} \leftarrow \sigma_{c3} + \Delta\sigma_{c3}$$

STEP 4: The new lateral stresses, resulting from step 3, do not satisfy the stress boundary conditions. That is, $\sigma'_2 + n_c\sigma_{c2} \neq \sigma_2$ and $\sigma'_3 + n_{c3} \neq \sigma_3$, where the global stresses σ_2 and σ_3 are the known confinement pressures. The strain ε_1, on the other hand, is calculated correctly.

STEP 5: Apply a stress correction through the iterations: $\Delta\sigma_2 = \sigma_2 - (\sigma'_2 + n_c\sigma_{c2})$ and $\Delta\sigma_3 = \sigma_3 - (\sigma'_3 + n_{c3})$, while $\Delta\varepsilon_1 = 0$, until the calculated correction values $\Delta\sigma_2$ and $\Delta\sigma_3$ are small enough.

The procedure described here is necessary to ensure equilibrium between the mixture components and the externally applied load. In a finite element solution, this step should be incorporated within the Newton equilibrium iterations to avoid additional computational burdens.

Radial mapping return

The integration of the constitutive equations of each phase in this multi-phase analysis is similar to that of a single-phase material. This means that during loading, each phase must satisfy the consistency condition of plasticity and maintain the stress tensor *on* its loading surface. Note that even though all phases have the same total strain tensor, they do not share the same elastic and plastic components. These are calculated individually for each phase.

The integration scheme adopted in this analysis is based on the generalized trapezoidal rule.[20] The mathematics of the algorithm is well established and will not be repeated here. A detailed presentation is found in Abdulla's[17] dissertation.

VERIFICATION

A large number of triaxial tests were performed on specimens with 2, 4 and 6 per cent cementation.[1] The ability of the proposed model to predict the behaviour of cemented soils is judged based on this data set. The material parameters were derived from triaxial tests on clean sand, and unconfined compression tests on cemented sand. Thus, the ability of this model to predict the behaviour of cemented sands under confinement, does not test only the 'multidimensional curve-fitting' ability of the model, but also the micromechanical concepts that are developed here. Figures 5–14 show the comparison between experimental and theoretical results for specimens with 2, 4 and 6 per cent cementation and confining pressures of 200 kPa (29 psi) and 300 kPa (43·5 psi).

The qualitative predictions of the model are considered excellent. The largest quantitative discrepancies were observed for the 2 per cent cemented specimens, where the model predicted a 'stiffer' early response. This is attributed partly to the experimental difficulties encountered with the 2 per cent cemented specimens. These specimens were manufactured, unintentionally, looser than the clean sand and the 4 and 6 per cent cemented specimens. As a result, they did not have the expected stiffness. Inspection of the experimental results presented in the companion paper[1]

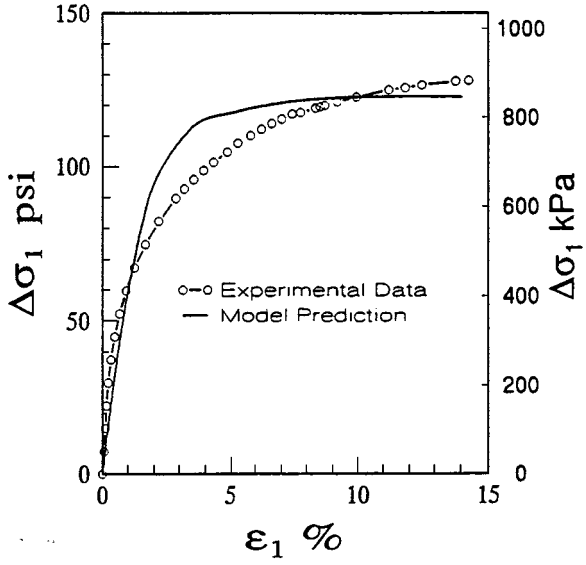

Figure 5. Experimental and theoretical shear response for the triaxial compression test for $\sigma_3 = 200$ kPa (29·0 psi). Cementation = 2%

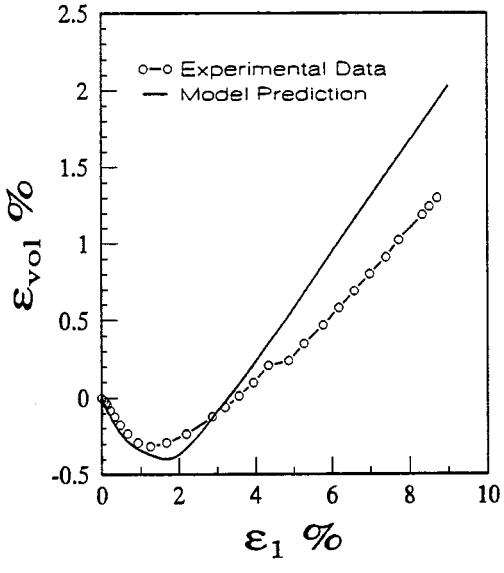

Figure 6. Experimental and theoretical volumetric response for the triaxial compression test for $\sigma_3 = 200$ kPa (29·0 psi). Cementation = 2%

reveals that the 2 per cent cemented specimens were more compliant than the pure sand specimens.

The shear response predictions for the 4 and 6 per cent cemented specimens, including softening due to bond breakage, are very good. The most impressive performance of the model,

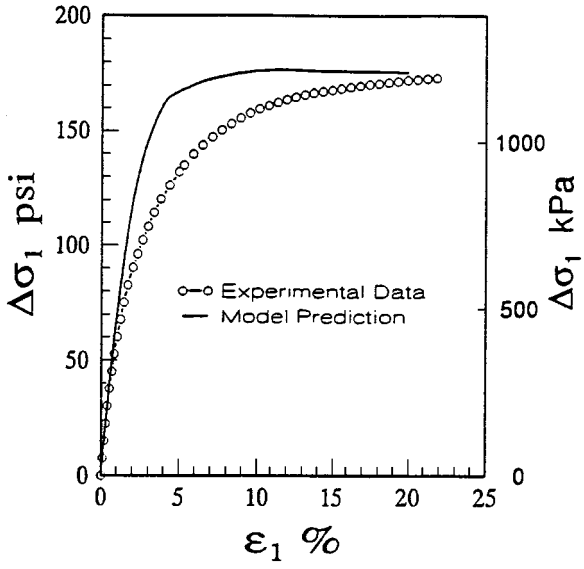

Figure 7. Experimental and theoretical shear response for the triaxial compression test for $\sigma_3 = 300$ kPa (43·5 psi). Cementation = 2%

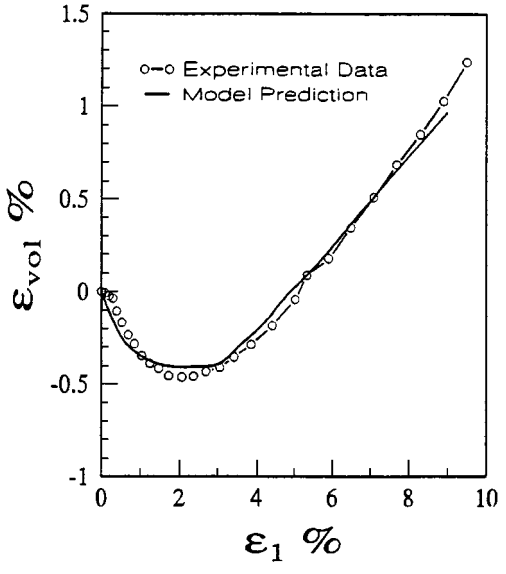

Figure 8. Experimental and theoretical volumetric response for the triaxial compression test for $\sigma_3 = 300$ kPa (43·5 psi). Cementation = 2%

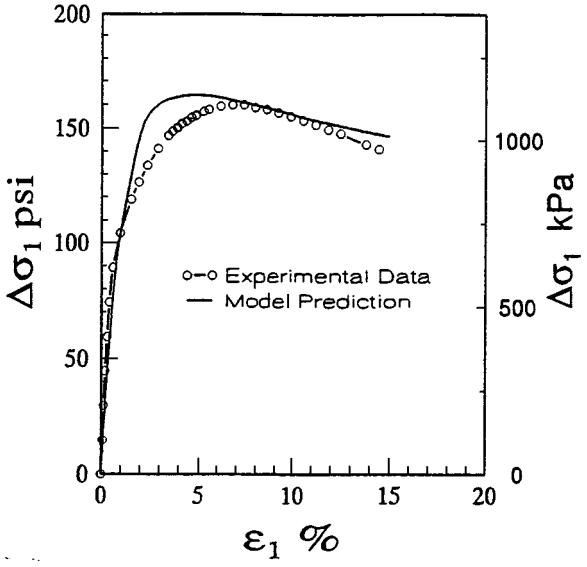

Figure 9. Experimental and theoretical shear response for the triaxial compression test for $\sigma_3 = 200$ kPa (29·0 psi). Cementation = 4%

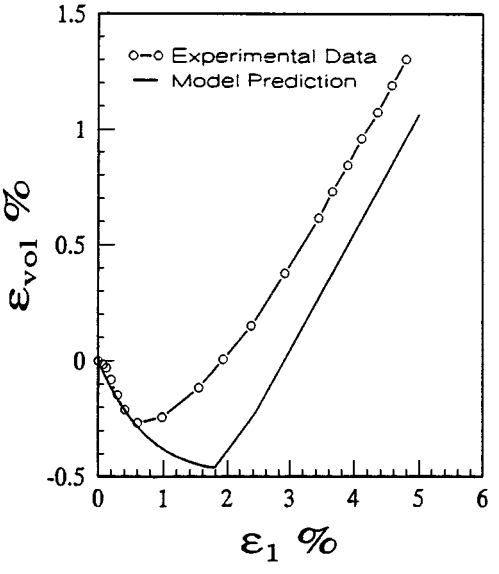

Figure 10. Experimental and theoretical volumetric response for the triaxial compression test for $\sigma_3 = 200$ kPa (29·0 psi). Cementation = 4%

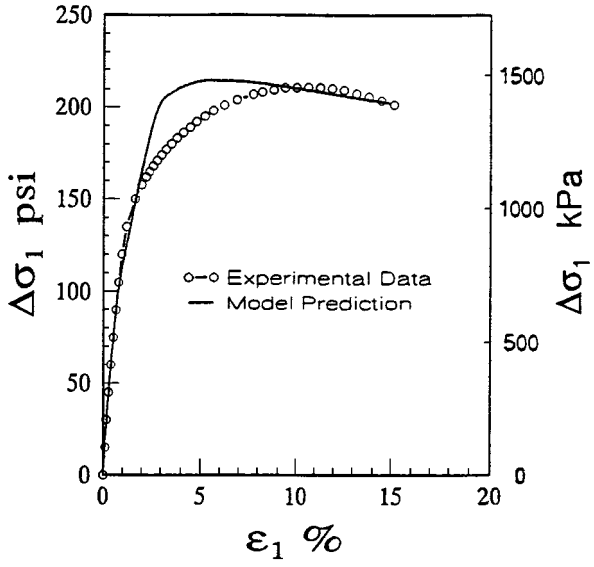

Figure 11. Experimental and theoretical shear response for the triaxial compression test for $\sigma_3 = 300$ kPa (43·5 psi). Cementation = 4%

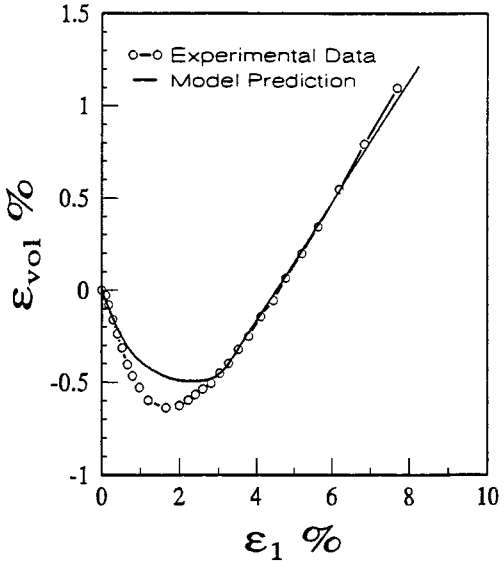

Figure 12. Experimental and theoretical volumetric response for the triaxial compression test for $\sigma_3 = 300$ kPa (43·5 psi). Cementation = 4%

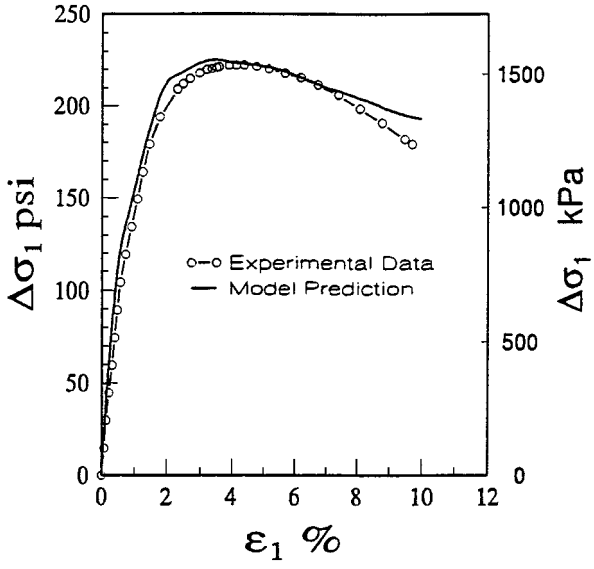

Figure 13. Experimental and theoretical shear response for the triaxial compression test for $\sigma_3 = 200$ kPa (29·0 psi). Cementation = 6%

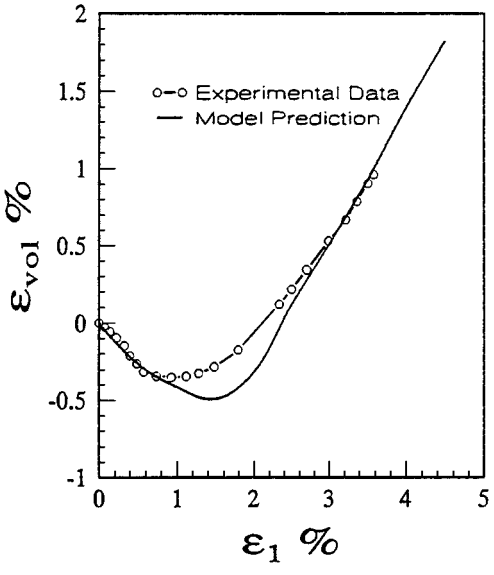

Figure 14. Experimental and theoretical volumetric response for the triaxial compression test for $\sigma_3 = 200$ kPa (29·0 psi). Cementation = 6%

however, is observed in the dilatation predictions, considering the physical complexities that govern the phenomenon.

DISCUSSION AND CONCLUSIONS

The multi-phase micromechanical approach to the modelling of cemented soils provides a theoretically sound basis for the analysis of cemented soils. Fairly simple plasticity models for the individual phases are combined to produce the mixture model that is presented here. Even though fewer material parameters could be desired, it is noted that all parameters are calculated from simple triaxial tests on clean sand, and uniaxial compression tests on cemented sand.

An important issue that should be addressed here is that of modelling naturally cemented soils, where the individual components may not be as clearly known. The testing and modelling procedures in such cases do not change. The soil parameters can be obtained by testing the soil that results from the complete breakage of the internal bonds of the natural soil, while the cementation properties can be obtained from unconfined testing of the undisturbed cemented soil. The exact percentage of cementation of a naturally cemented soil is not known usually, but this does not constitute a serious problem. A study conducted by the authors on the cementation modelling indicate that calculations based on assumptions of 4 per cent cementation, or 6 per cent cementation of the same soil (with actual cementation 4 per cent) gave the same stress–strain predictions when the appropriate strength adjustments were made. *Appropriate strength adjustments* simply means that an increase of the assumed value of cementation means larger assumed n_{c0} (equation (44)), and subsequently smaller calculated values of α_c^0 and α_c^{ult} (equations (45) and (46)). In other words, it is mathematically equivalent to assume smaller amount of cementation with larger strength, or larger amount of cementation with smaller strength.

Finally, the variable cement content expressed by n_c is a very efficient measure of the material degradation or damage, and should prove valuable in future studies related to the stability of cemented sands.

REFERENCES

1. A. A. Abdulla and P. D. Kiousis, 'Behavior of cemented soils; Part I: Testing', *Int. j. numer. analyt. methods geomech.*, **21,** 533–547 (1997).
2. S. K. Saxena and R. M. Lastrico, 'Static properties of lightly cemented sand', *J. Geotech. Eng. Div. ASCE*, **104,** 1449–1464 (1978).
3. S. Frydman, D. Hendron, H. Horn, J. Steinbach, R. Baker and B. Shaal, 'Liquefaction study of cemented sands', *J. Geotech. Eng. Div. ASCE*, **106,** 275–297.
4. N. Sitar, G. W. Clough and R. C. Bachus, 'Behavior of weakly cemented soil slopes under static and seismic loading conditions', *Report No. 44*, The John A. Blume Earthquake Engineering Center, Stanford University, Stanford, CA, 1980.
5. R. C. Bachus, G. W. Clough, N. Sitar, N. S. Rad, J. Crosby and P. Kaboli, 'Behavior of weakly cemented soil slopes under static and seismic loading conditions', *Report No. 52*, Vol. 2, The John A. Blume Earthquake Engineering Center, Stanford University, Stanford, CA, 1981.
6. T. D. O'Rourke and E. Crespo, 'Geotechnical properties of cemented volcanic soil', *J. Geotech. Eng. ASCE*, **114,** 1126–1147 (1988).
7. P. V. Lade and D. D. Overton, 'Cementation effects in frictional materials', *J. Geotech. Eng. ASCE*, **115,** 1373–1387 (1989).
8. P. D. Kiousis and A. A. Abdulla, 'Associative plasticity for dilatant soils', *J. Eng. Mech.* **118,** 763–785 (1992).
9. P. V. Lade, 'Elastoplastic stress–strain theory for cohesionless soil', *J. Geotech. Eng. Div. ASCE* **101,** 1037–1053.
10. C. S. Desai, S. Somasundaram and G. Frantziskonis, 'A hierarchical approach for constitutive modeling of geologic materials', *Int. j. numer. analyt. methods geomech.*, **10,** 225–257 (1986).

11. S. Sture, H.-J. Ko and J. C. Mould, 'Elastic-plastic anisotropic hardening model and prediction of behavior for dry quartz sand', in G. Gudehus, F. Darve and I. Vardoulakis (eds), *Constitutive Relations for Solids*, A. A. Balkema, Rotterdam, The Netherlands, 1982 pp. 227–248.
12. H. Hirai, M. Takahashi and M. Yamada, 'An elastic-plastic constitutive model for the behavior of improved sandy soils', *Soils Found*., **29,** 69–84 (1989).
13. O. A. Pekau and V. Gocevski, 'Elasto-plastic model for cemented and pure sand deposits', *Comput. Geotech*., **7,** 155–187 (1989).
14. C. S. Desai, S. V. Jagannath and T. Kundu, 'Mechanical and ultrasonic response of soil', *J. Eng. Mech. ASCE*, **121,** pp. 744–752 (1995).
15. C. S. Desai and J. Toth 'Disturbed state constitutive modeling based on stress–strain and nondestructive behaviors', *Int. J. Solids Struct*., **33,** pp. 1619–1650 (1996).
16. R. D. Holtz and W. D. Kovacs, *An Introduction to Geotechnical Engineering*, Prentice-Hall, Inc., Englewood Cliffs, NJ, 1981.
17. A. A. Abdulla, 'Testing and constitutive modeling of cemented soils', *Dissertation*, University of Arizona at Tucson, AZ 1992.
18. N. Janbu, 'Soil compressibility as determined by oedometer and triaxial tests', *European Conf. on Soil Mechanics and Foundation Engineering*, Wissbaden, Germany, Vol. 1, 1963. pp. 19–25.
19. G. W. Clough, N. Sitar, R. C. Bachus and N. S. Rad, 'Cemented sands under static loading', *J. Geotech. Eng. Div. ASCE*, **107,** 799–817 (1981).
20. M. Ortiz and E. P. Popov, 'Accuracy and stability of integration algorithms for elastoplastic constitutive relations', *Int. j. numer. methods Eng*., **21,** 1561–1576 (1985).

